NACA RM L52L29

NACA

RESEARCH MEMORANDUM

AN EXPERIMENTAL INVESTIGATION OF BOUNDARY INTERFERENCE ON FORCE AND MOMENT CHARACTERISTICS OF LIFTING MODELS IN THE LANGLEY 16- AND 8-FOOT TRANSONIC TUNNELS

By Charles F. Whitcomb and Robert S. Osborne

Langley Aeronautical Laboratory
Langley Field, Va.

NATIONAL ADVISORY COMMITTEE
FOR AERONAUTICS
WASHINGTON

February 24, 1953
Declassified February 9, 1956

NATIONAL ADVISORY COMMITTEE FOR AERONAUTICS

RESEARCH MEMORANDUM

AN EXPERIMENTAL INVESTIGATION OF BOUNDARY INTERFERENCE ON FORCE AND MOMENT CHARACTERISTICS OF LIFTING MODELS IN THE LANGLEY 16- AND 8-FOOT TRANSONIC TUNNELS

By Charles F. Whitcomb and Robert S. Osborne

SUMMARY

A wing-fuselage force model configuration and the fuselage alone have been tested at angles of attack up to 32° in the Langley 16-foot transonic tunnel. The force and moment characteristics obtained from these tests are presented with comparable measurements obtained from previous tests of the identical model and with a model geometrically similar but three times as large in the Langley 8-foot and 16-foot transonic tunnels, respectively. The agreement of the compared results indicates that boundary-interference effects are of small magnitude for the particular configurations tested.

INTRODUCTION

The investigation of the accuracy and reliability of aerodynamic data obtained from transonic wind tunnels involves four major problems. These problems are: (1) tunnel-flow uniformity, (2) blockage, (3) lift interference, and (4) at supersonic speeds, the reflection of disturbances from the test-section boundary. The reduction of solid blockage interference by a slotted-wall test section was reported in reference 1. In these tests, closed tunnel choking was eliminated and low supersonic velocities were attained. The attainment of improved flow uniformities in this tunnel is described in reference 2. Based on these results, the Langley 8-foot and 16-foot tunnels were modified to slotted transonic tunnels, and the calibration results of these tunnels as presented in references 3 and 4, respectively, indicated the attainment of uniform flows. Comparisons of pressure-distribution results from tests on nonlifting models in these tunnels with those from free-fall tests (refs. 3 and 5) showed negligible tunnel interference effects at subsonic

speeds and small though significant interference due to boundary-reflected disturbances at low supersonic speeds.

The tunnel boundary effects on lifting-model characteristics obtained in slotted test sections have been the subject of recent investigation. Unpublished theoretical solutions in the subsonic range show that for model sizes currently tested in these tunnels, the corrections to the lift-curve slope may be neglected. Reference 6 provides an experimental indication of tunnel-wall effects on reflection-plane model lifting wings in a slotted tunnel. Other currently available data (ref. 7) indicate that under some conditions of testing the effects of boundary-reflected disturbances at supersonic speeds may be voided by interpretation of test results.

Some additional information concerning boundary-interference effects in slotted tunnels on force and moment characteristics of lifting models has been made available by the completion of a series of tests of typical transonic wing-fuselage and fuselage-alone models in the Langley 16-foot and 8-foot transonic tunnels. A wing-fuselage configuration and the fuselage alone, typical of the size tested in the 8-foot tunnel, have been tested in both the 8-foot (ref. 7) and 16-foot tunnels. Also, a geometrically similar wing-fuselage model, typical in size of 16-foot tunnel models (three times the size of the model tested in the 8-foot tunnel), has been tested in the 16-foot tunnel (ref. 8). The present paper describes the tests of the smaller model in the 16-foot tunnel and presents the resultant force and moment characteristics as comparisons with the previously published information. These comparisons provide information on the boundary interference including the effects of both the lifting interference and the reflected disturbances on sting-mounted lifting models tested in the Langley 8-foot and 16-foot transonic tunnels.

SYMBOLS

C_D	drag coefficient, D/qS
C_L	lift coefficient, L/qS
C_m	pitching-moment coefficient, $M_{\bar{c}/4}/qS\bar{c}$
$\bar{c}$	wing mean aerodynamic chord
D	drag, lb
L	lift, lb
M	Mach number

$M_{\bar{c}/4}$ pitching moment about $\bar{c}/4$, in-lb

P_b base pressure coefficient, $\frac{p_b - p_o}{q}$

p_o free-stream static pressure, lb/sq ft

p_b static pressure at model base, lb/sq ft

q free-stream dynamic pressure, $\frac{1}{2}\rho V^2$, lb/sq ft

R Reynolds number based on $\bar{c}$

S wing area, sq ft

V free-stream velocity, ft/sec

α angle of attack of fuselage center line, deg

ρ free-stream density, slugs/cu ft

APPARATUS AND TESTS

The present tests were made in the Langley 16-foot transonic tunnel (ref. 4). The model, its three-component internal electrical strain-gage balance, and the 18-inch portion of the support sting immediately rearward of the model were the same as tested in the Langley 8-foot transonic tunnel and reported in reference 7. The wing was mounted on the fuselage center line and had 45° sweepback referred to the quarter-chord line, a taper ratio of 0.60, an aspect ratio of 4, and NACA 65A006 airfoil sections parallel to the free stream. The fuselage was designed by cutting off the rearward portion of a body of revolution with a fineness ratio of 12 to form a body with a fineness ratio of approximately 10. Both the wing and fuselage were made of steel. Dimensional details of the model are given in figure 1; ordinates of the airfoil section and the fuselage are available in reference 7. A static orifice located at the side of the support sting in the plane of the model base was used to measure the base pressure.

At its downstream end, the balance sting was attached to the tunnel support sting by means of angular couplings used to augment the pitch-attitude range of the support system which normally has a maximum limit of 15° (see ref. 8).

Shadowgraph pictures of the air stream in the vicinity of the model were obtained using an f:2.5 lens and a shutter speed of 1/150 second.

A mercury-arc diverging-light supply placed in the horizontal plane passing through the tunnel center line was directed normal to the air stream at the midsection of the body.

The model used for the tests of reference 8 was geometrically similar to the model just described, but was three times as large. The ratio of sting diameter at the plane of the model base to model-base diameter was approximately equal to that for the smaller model. It was also of similar construction, thus minimizing the effects of aeroelasticity on the data comparison.

The smaller wing-fuselage model as tested in the 16-foot and 8-foot tunnels will be referred to hereinafter as the small model, and the model that is three times as large and tested in the 16-foot tunnel will be referred to as the large model. Dimensions of the models and the tunnel test sections are given in table I.

The variation with Mach number of test Reynolds number based on the wing mean aerodynamic chord is presented in figure 2. Lift, drag, and pitching moment were measured for the wing-fuselage combination and the fuselage alone at several angles of attack over a Mach number range from 0.60 to approximately 1.07. Accuracies of the presented lift, drag, and pitching-moment coefficients are estimated to be within ±0.02, ±0.002, and ±0.004, respectively. Test-section Mach number accuracy for both the 16-foot and 8-foot transonic tunnels was ±0.005. The model angles as presented are estimated to be accurate to ±0.15°. No corrections have been applied to any of the data presented.

RESULTS AND DISCUSSION

Force and Moment Characteristics

Lift, drag, and pitching-moment data from tests of the wing-fuselage models are presented as functions of angle of attack or lift coefficient in figures 3 to 5. Figures 6 to 8 present the model characteristics as a function of Mach number. Comparisons of the small-model fuselage-alone characteristics as obtained from tests in the Langley 16-foot and 8-foot transonic tunnels are presented in figures 9 and 10. Experimental points have been presented wherever possible, and faired data are used to complete the comparisons.

Wing fuselage at subsonic speeds.- The evaluation of possible boundary-interference effects on typical model test results in the 16-foot and 8-foot transonic tunnels over the subsonic Mach number range is accomplished by comparisons with the force and moment results obtained from the small model tested in the 16-foot tunnel, which are assumed to

be essentially interference free. This assumption is considered reasonable since the ratio of maximum cross-sectional area of model to cross-sectional area of tunnel is only about 0.0004 (see table I). These comparisons (figs. 3 to 8) indicate generally small differences over the low and medium lift range represented by the approximately straight line part of the lift curve. The occasional somewhat greater differences in the data at low Mach numbers represent random experimental error and are therefore not significant. More appreciable discrepancies occur above an angle of attack and lift coefficient of $\alpha = 8^{\circ}$ and $C_L = 0.6$, respectively, at which conditions the lift-curve slopes decrease, indicating the spread of flow separation over the wing-tip sections. The flow over the small leading-edge-radius highly swept wing in this high angle-of-attack range is known to be very sensitive to model surface and stream turbulence conditions, making repeatability of test results difficult.

These results seem to indicate, even at the higher angles of attack, that subsonic boundary-interference effects on the total force and moment characteristics are shown to be small for the wing-fuselage combinations represented herein when tested in the 16-foot and 8-foot transonic tunnels.

Wing fuselage at supersonic speeds.- Boundary interference is known to exist in the low supersonic Mach number range of slotted-test-section transonic tunnels. Briefly, the presence of the tunnel boundary located a finite distance from the test model permits flow disturbances which originate in the stream at the forward sections of the model to be reflected back onto the more rearward portions of the model. At Mach numbers high enough to sweep these reflections downstream of the model base, the test results are considered completely free of interference. For the present tests the boundary-interference-free condition for the small model in the 16-foot tunnel is estimated, by use of shadowgraph pictures presented later in this paper, to begin at a Mach number of about 1.045. At lower supersonic speeds the axial forces appear to be appreciably influenced by boundary-reflected disturbances only at Mach numbers slightly greater than 1.0 (fig. 7(b)). These findings are in agreement with those reported in reference 3. Therefore, in consideration of these observations, the 16-foot transonic tunnel test results for the small model provide an essentially interference-free basis for evaluating the extent of interference effects on the other data except at Mach numbers only slightly greater than 1.0.

The supersonic characteristics of the wing-fuselage configurations tested in the two tunnels are compared in figures 3 to 8. In general, the indicated differences over the supersonic Mach number range are of slight magnitude, although differences as large as 0.02, 0.008, and 0.014 in lift, drag, and pitching-moment coefficients, respectively, occur at angles of attack of 8° or larger. It is to be noted that the general trends of the force and moment characteristics are similar for the

several tests as a function of angle of attack or lift coefficient. The consistent small displacements of the curves may be due to the effects of boundary-reflected disturbances in combination with possible effects of other factors such as Reynolds number, separation, and experimental error.

In general, the comparisons of the results obtained from the wing-fuselage models tested at lifting attitudes in the two tunnels are indicative of small boundary-interference effects over the entire Mach number range investigated. These results should be applied to other tests with caution, however, and only after careful consideration of the particular configuration involved. For example, a configuration with a conventional horizontal tail or with a large portion of the lifting surface well downstream of the nose might have the pitching-moment data seriously affected by the boundary-reflected disturbances.

Fuselage alone.- The force and moment characteristics of the small-model fuselage-alone tests in the two tunnels are compared in figures 9 and 10 for varying angle of attack and Mach number, respectively. In general, the compared data were in good agreement. An exception occurred in the low supersonic Mach number range, where boundary-reflected disturbances resulted in drag-coefficient differences as large as 0.003 at a Mach number of 1.04. Although such a drag increment is not large, it is significant since it represents a sizeable percentage of the total body drag. The fuselage-alone drag differences are of approximately the same magnitude as the differences which occurred for the small wing-fuselage model comparisons over a similar angle-of-attack and Mach number range (see fig. 7(b)). Therefore, since the differences for the wing-fuselage tests are no greater than for the fuselage alone, it appears that drag of the wing has not been affected by the reflected disturbances.

Base Pressures

Base-pressure-coefficient results of the small-model wing-fuselage and fuselage-alone configurations tested in the two tunnels are presented as a function of Mach number in figure 11. The comparisons indicate some slight differences in the form of the curves in the compared supersonic range which are attributed to the passing of the reflected expansions and compressions over the regions of the model base.

Shadowgraph Pictures

Shadowgraph pictures of the small-model wing-fuselage and fuselage-alone configurations tested at several angles of attack and at transonic Mach numbers in the 16-foot tunnel are presented in figures 12 and 13. In the low supersonic speed range, increases in the model angle of attack

caused the wing leading-edge root-juncture shocks to become stronger and more normal to the stream (see fig. 12). The fuselage nose shocks were similarly affected to a smaller degree. At a Mach number of 1.03 (fig. 12(e)) increasing the angle of attack to 12.3° caused the wing leading-edge root-juncture shock to become sufficiently strong to leave the vicinity of the wing and combine with the fuselage nose shock. (At the higher angles in figs. 12(e) and 12(f), the normal disturbances pictured immediately behind the wing leading-edge root-juncture and fuselage-nose shocks are merely the intersection line of these shocks with the tunnel-wall window.)

CONCLUDING REMARKS

Tests of a fuselage-alone and of wing-fuselage configurations having model-to-tunnel cross-sectional-area ratios from 0.0003 to 0.0038 have been conducted in the slotted test sections of the Langley 16-foot and 8-foot transonic tunnels in order to obtain experimental information concerning the effects of boundary interference on force and moment characteristics of typical models at lifting attitudes for Mach numbers from 0.60 to 1.07. The agreement of the test results indicated that boundary-interference effects on the force and moment characteristics of these models were small.

Langley Aeronautical Laboratory,
National Advisory Committee for Aeronautics,
Langley Field, Va.

REFERENCES

1. Wright, Ray H., and Ward, Vernon G.: NACA Transonic Wind-Tunnel Test Sections. NACA RM L8J06, 1948.

2. Ward, Vernon G., Whitcomb, Charles F., and Pearson, Merwin D.: An NACA Transonic Test Section With Tapered Slots Tested at Mach Numbers to 1.26. NACA RM L50B14, 1950.

3. Ritchie, Virgil S., and Pearson, Albin O.: Calibration of the Slotted Test Section of the Langley 8-Foot Transonic Tunnel and Preliminary Experimental Investigation of Boundary-Reflected Disturbances. NACA RM L51K14, 1952.

4. Ward, Vernon G., Whitcomb, Charles F., and Pearson, Merwin D.: Air-Flow and Power Characteristics of the Langley 16-Foot Transonic Tunnel With Slotted Test Section. NACA RM L52E01, 1952.

5. Hallissy, Joseph M., Jr.: Pressure Measurements on a Body of Revolution in the Langley 16-Foot Transonic Tunnel and a Comparison With Free-Fall Data. NACA RM L51L07a, 1952.

6. Sleeman, William C., Jr., Klevatt, Paul L., and Linsley, Edward L.: Comparison of Transonic Characteristics of Lifting Wings From Experiments in a Small Slotted Tunnel and the Langley High-Speed 7- by 10-Foot Tunnel. NACA RM L51F14, 1951.

7. Osborne, Robert S., and Mugler, John P., Jr.: Aerodynamic Characteristics of a 45° Sweptback Wing-Fuselage Combination and the Fuselage Alone Obtained in the Langley 8-Foot Transonic Tunnel. NACA RM L52E14, 1952.

8. Hallissy, Joseph M., and Bowman, Donald R.: Transonic Characteristics of a 45° Sweptback Wing-Fuselage Combination. Effect of Longitudinal Wing Position and Division of Wing and Fuselage Forces and Moments. NACA RM L52K04, 1952.

TABLE I.- DIMENSIONS OF TUNNEL TEST SECTIONS AND MODELS

Tunnel Test Sections

Langley tunnels	Effective test-section diameter, ft	Test-section cross-sectional area, sq ft
16-foot transonic	15.95	199.9
8-foot transonic	7.30	42.9

Models

Model configuration	Maximum cross-sectional area, sq ft	Wing mean aerodynamic chord, ft	Wing area, sq ft	Fuselage length, ft
Small fuselage	0.061	-----	---	2.72
Small wing fuselage	.084	0.510	1.0	2.72
Large wing fuselage	.756	1.531	9.0	8.33

Ratios of Model-to-Tunnel Dimensions

Model-tunnel configuration	Ratio of model maximum cross-sectional area to tunnel-test-section cross-sectional area	Ratio of model wing plan-form area to tunnel-test-section cross-sectional area	Ratio of model fuselage length to tunnel-test-section effective diameter
Small fuselage model in 16-foot transonic tunnel	0.0003	------	0.1705
Small fuselage model in 8-foot transonic tunnel	.0014	------	.3725
Small wing-fuselage model in 16-foot transonic tunnel	.0004	0.0050	.1705
Small wing-fuselage model in 8-foot transonic tunnel	.0020	.0233	.3725
Large wing-fuselage model in 16-foot transonic tunnel	.0038	.0450	.5225

NACA

Wing Details

Airfoil section (parallel to plane of symmetry)	NACA 65A006
Area, sq ft	1
Aspect ratio	4
Taper ratio	0.6
Incidence, deg	0
Dihedral, deg	0

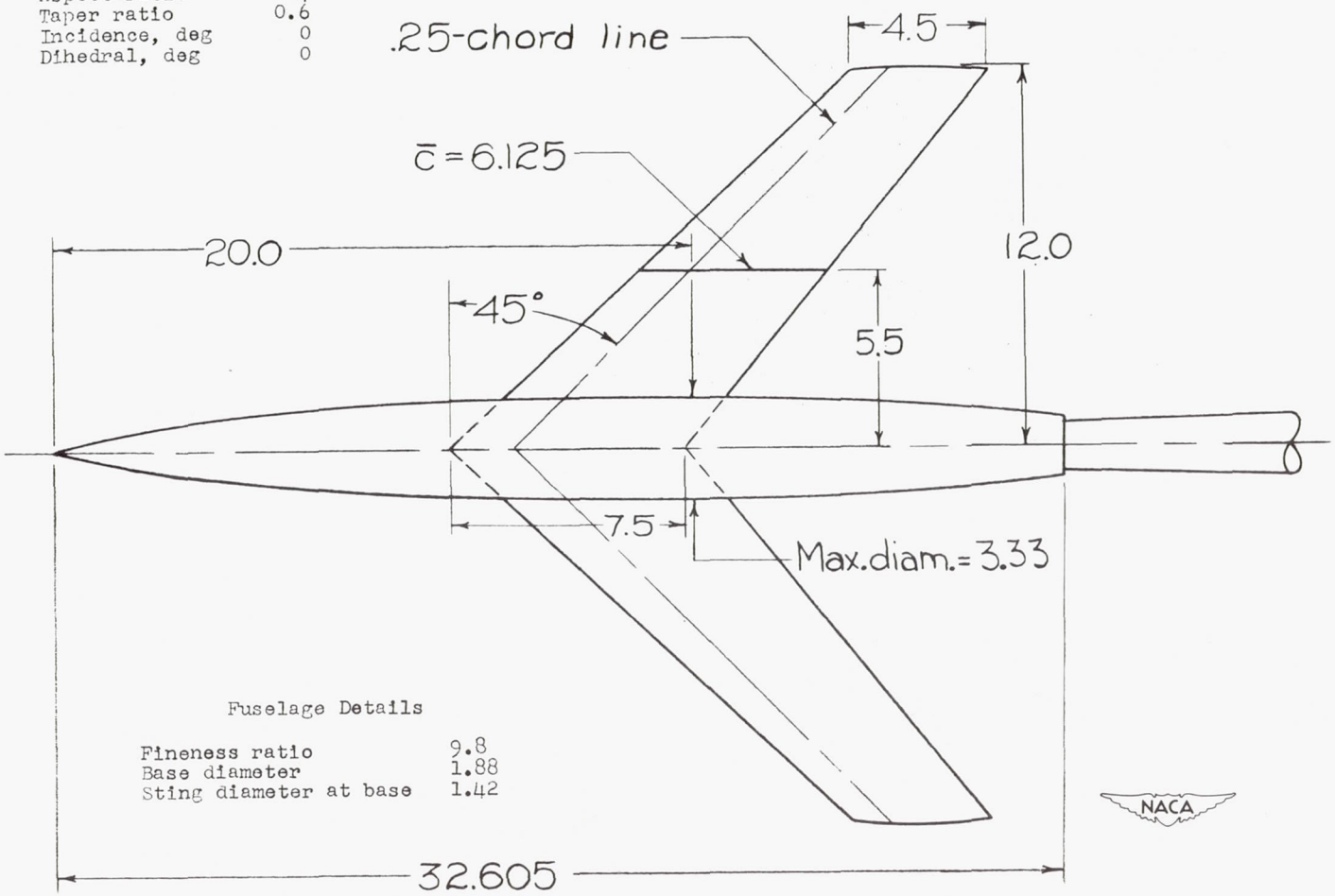

Fuselage Details

Fineness ratio	9.8
Base diameter	1.88
Sting diameter at base	1.42

Figure 1.- Model details. All dimensions in inches unless otherwise noted.

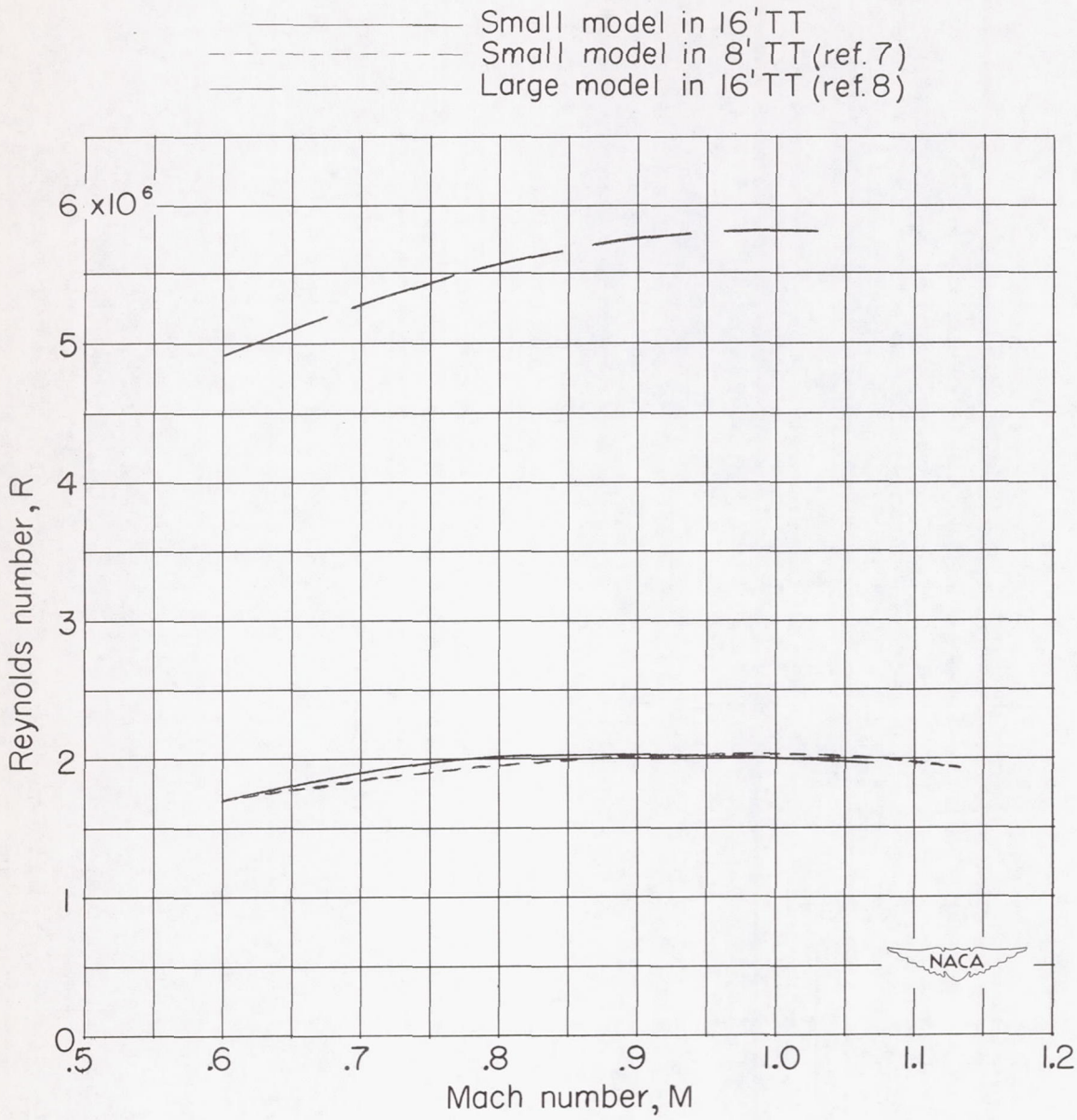

Figure 2.- Variation with Mach number of test Reynolds number based on the mean aerodynamic chord of the model wing.

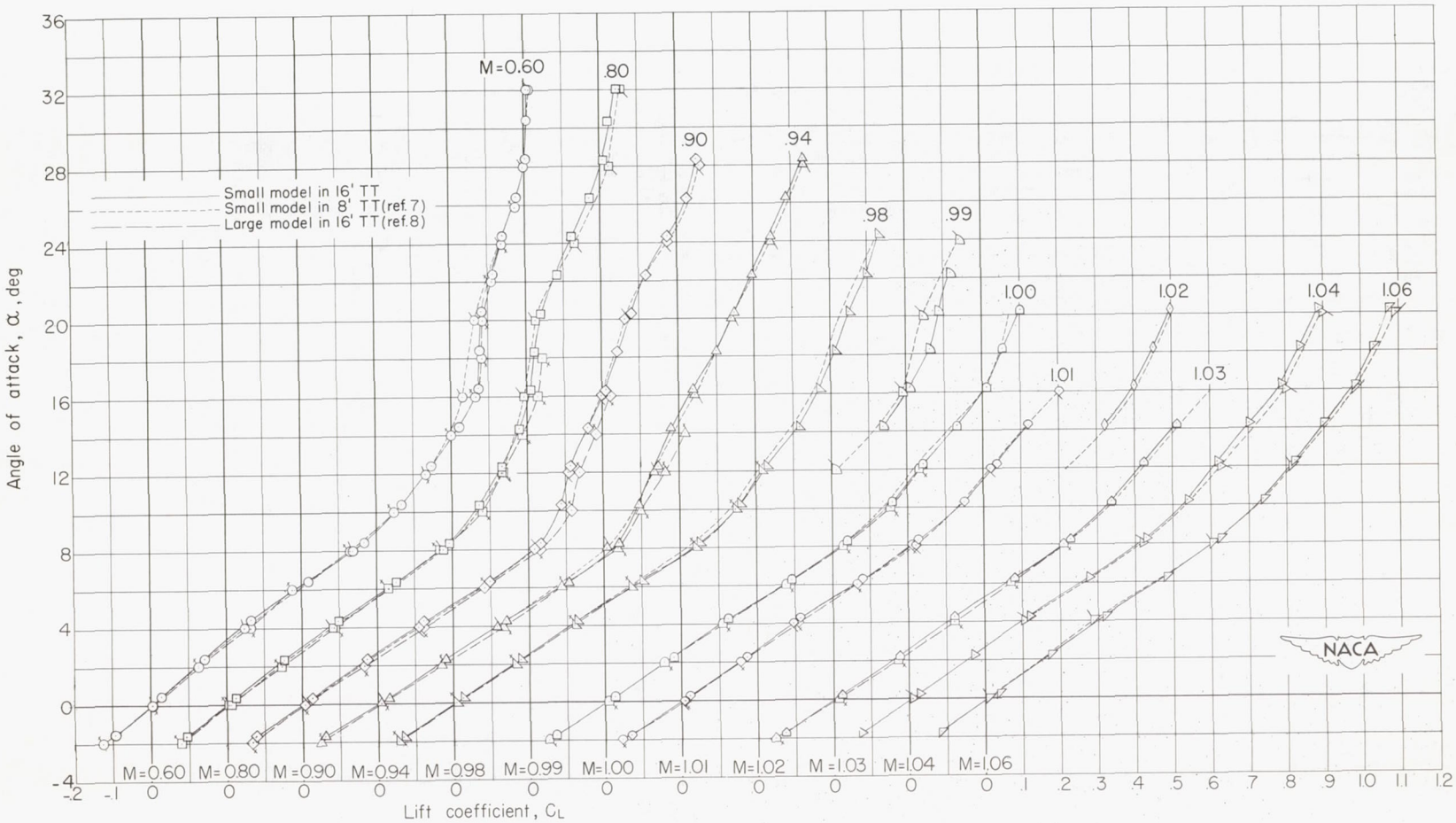

Figure 3.- Variation of angle of attack with lift coefficient for wing-fuselage configurations. (Plain and single flagged symbols indicate data from small model in Langley 16-foot and 8-foot transonic tunnels, respectively; cross-flagged symbols indicate data from large model in 16-foot transonic tunnel.)

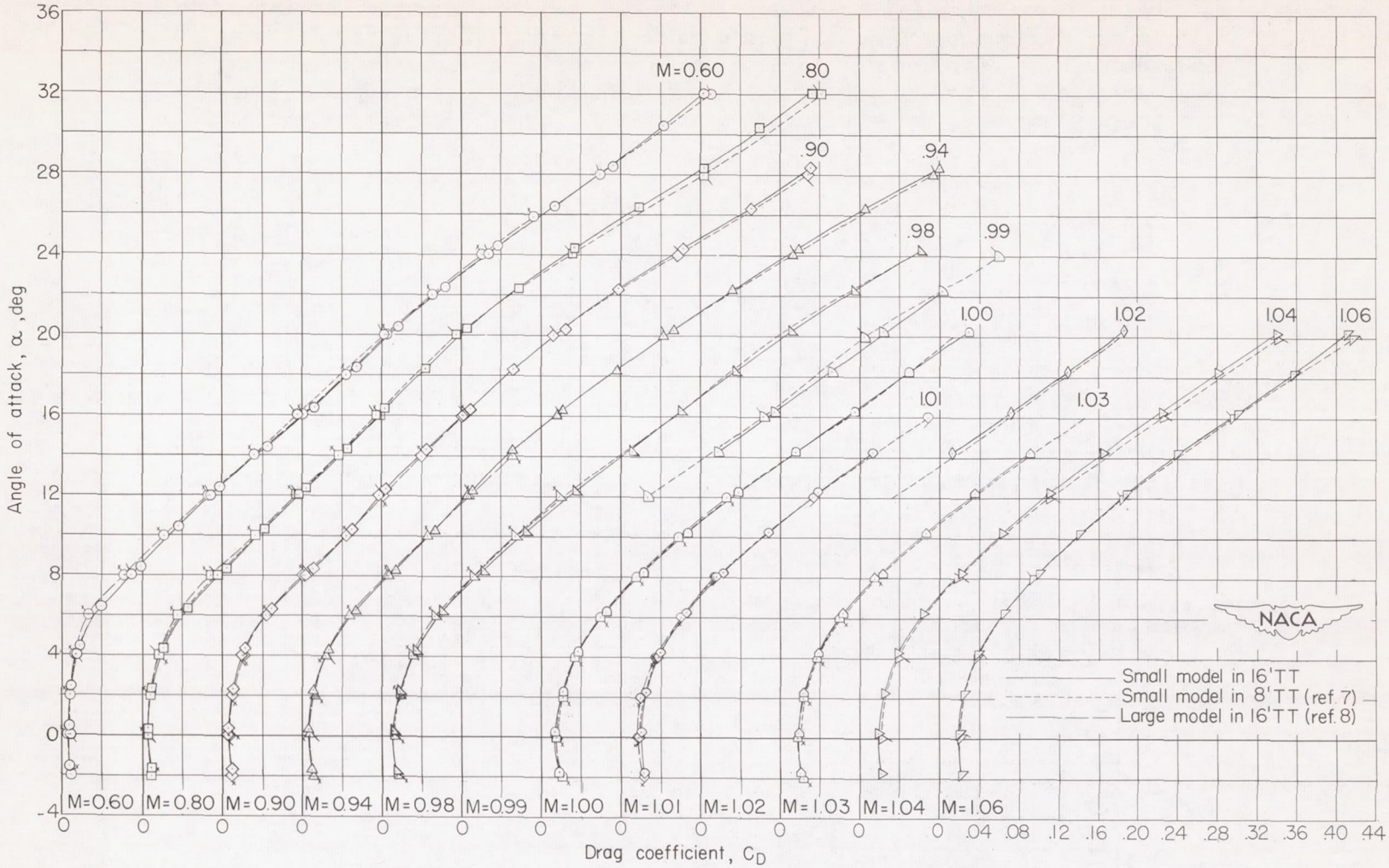

Figure 4.- Variation of angle of attack with drag coefficient for the wing-fuselage configurations. (Plain and single flagged symbols indicate data from small model in the Langley 16-foot and 8-foot transonic tunnels, respectively; cross-flagged symbols indicate data from large model in the 16-foot transonic tunnel.)

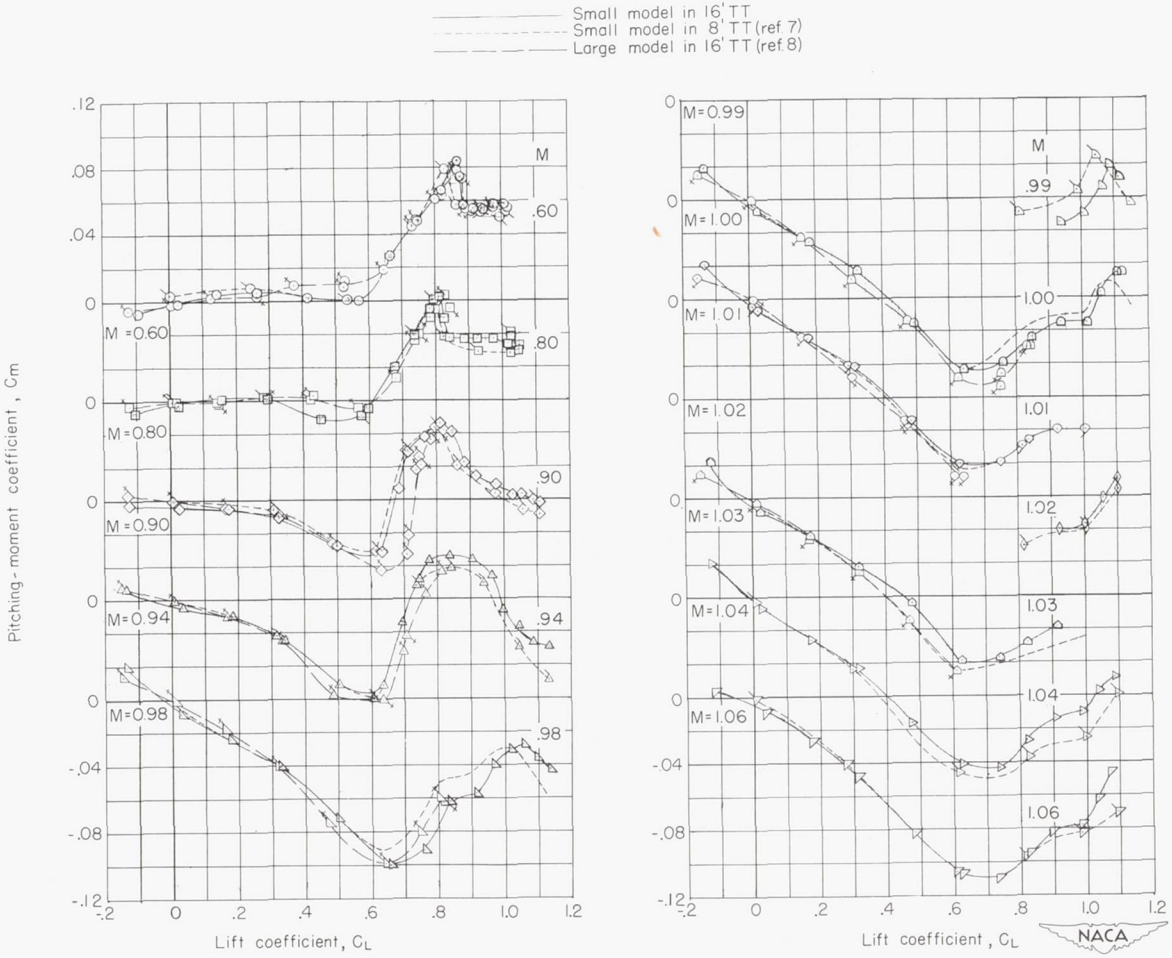

Figure 5.- Variation of pitching-moment coefficient with lift coefficient for the wing-fuselage configurations. (Plain and single flagged symbols indicate data from small model in the Langley 16-foot and 8-foot transonic tunnels, respectively; cross-flagged symbols indicate data from large model in 16-foot transonic tunnel.)

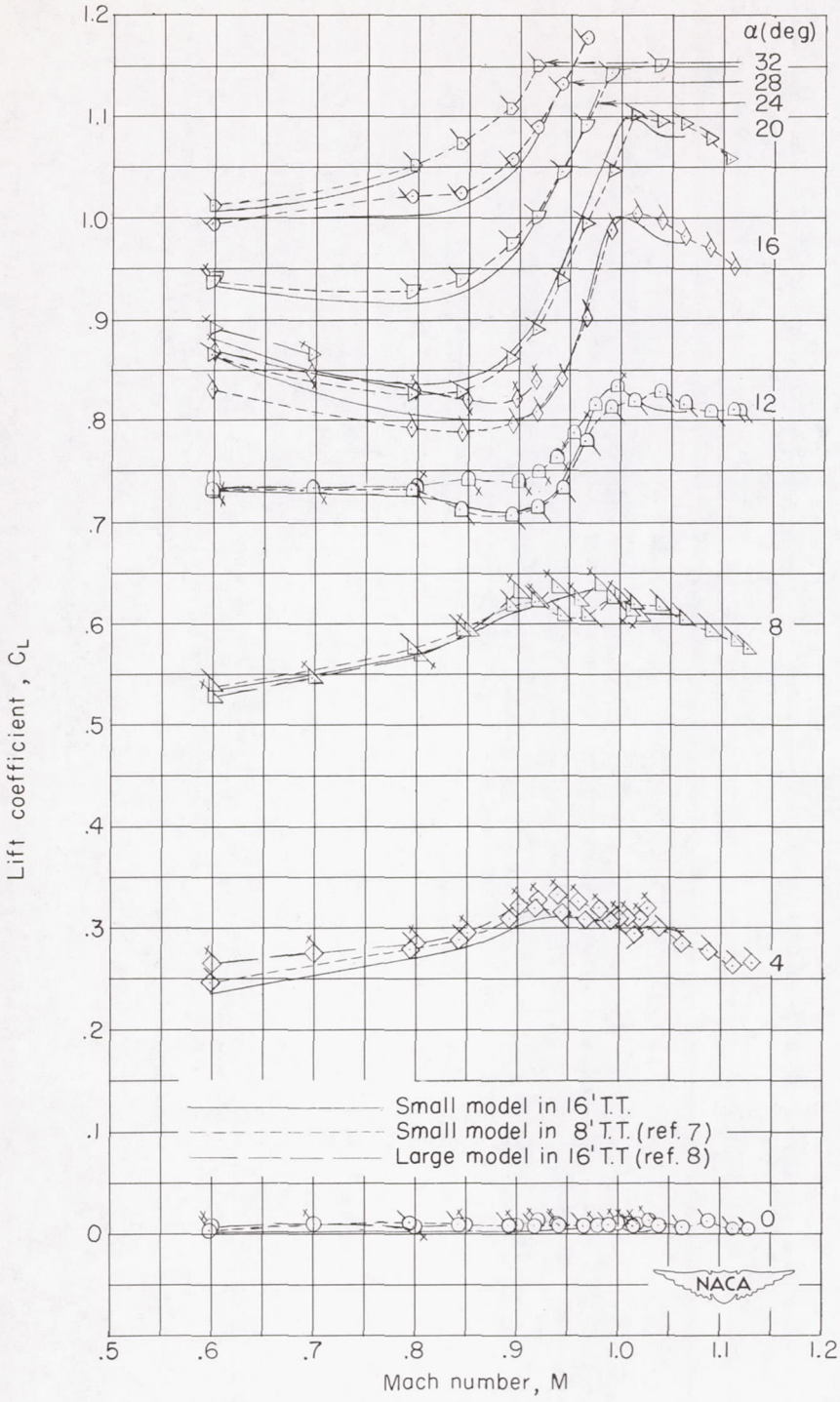

Figure 6.- Variation of lift coefficients with Mach number for the wing-fuselage configurations. (Single flagged symbols indicate data from small model in the Langley 8-foot transonic tunnel; cross-flagged symbols indicate data from large model in the Langley 16-foot transonic tunnel.)

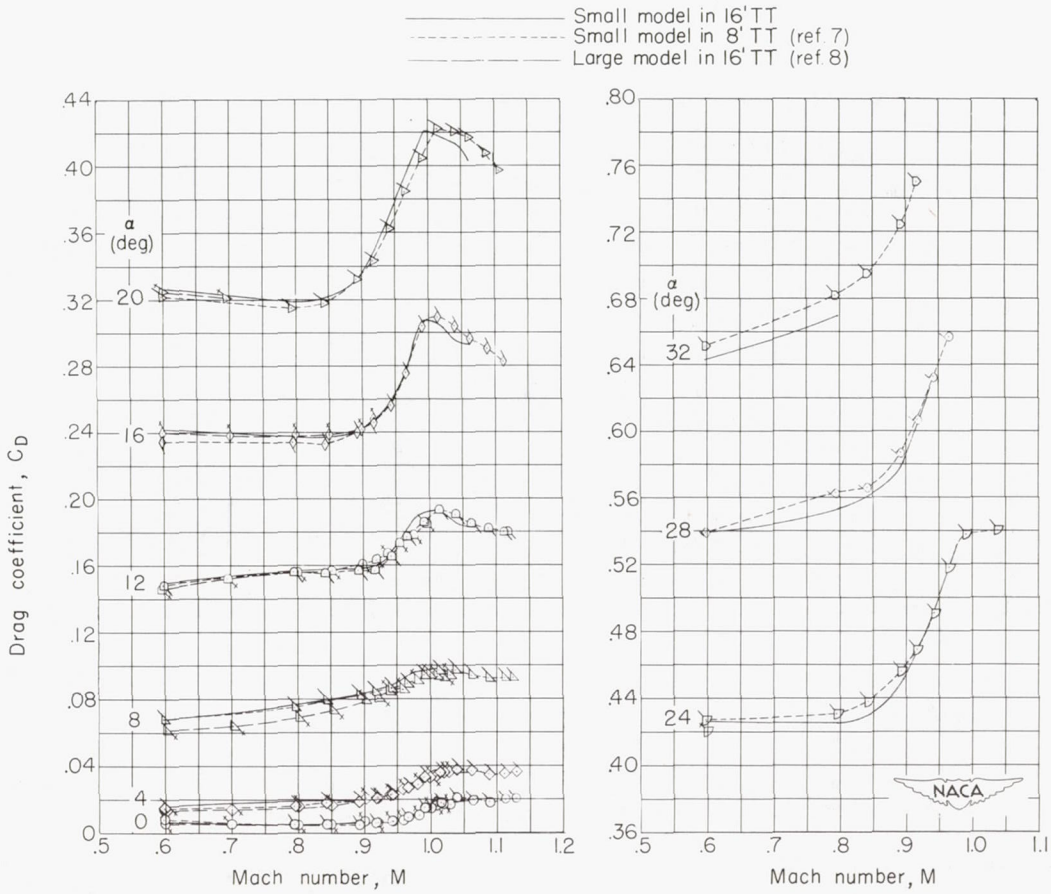

(a) Complete angle range.

Figure 7.- Variation of drag coefficient with Mach number for the wing-fuselage configurations. (Single flagged symbols indicate data from small model in the Langley 8-foot transonic tunnel; cross-flagged symbols indicate data from the large model in the Langley 16-foot transonic tunnel.)

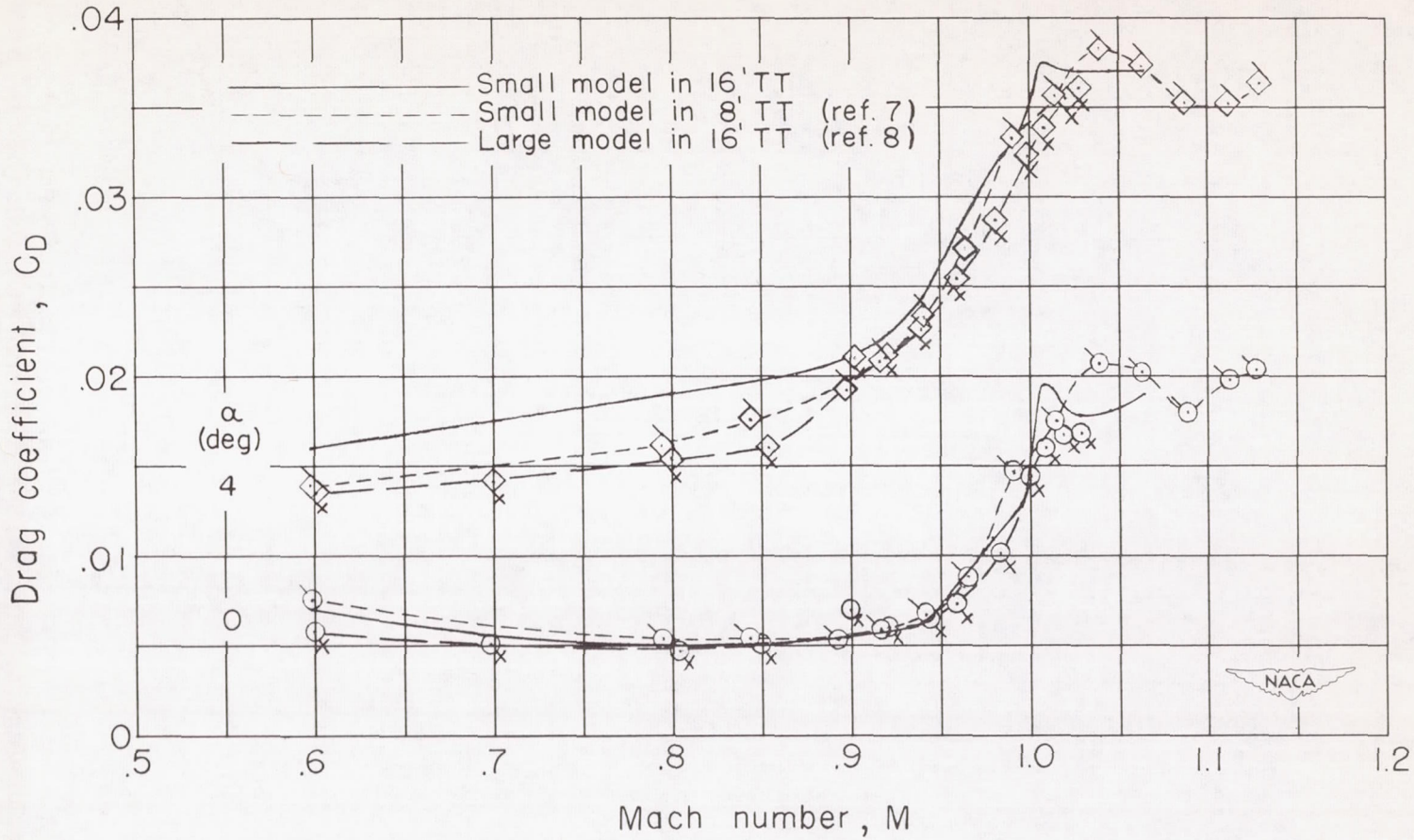

(b) $\alpha = 0^{\circ}; 4^{\circ}$.

Figure 7.- Concluded.

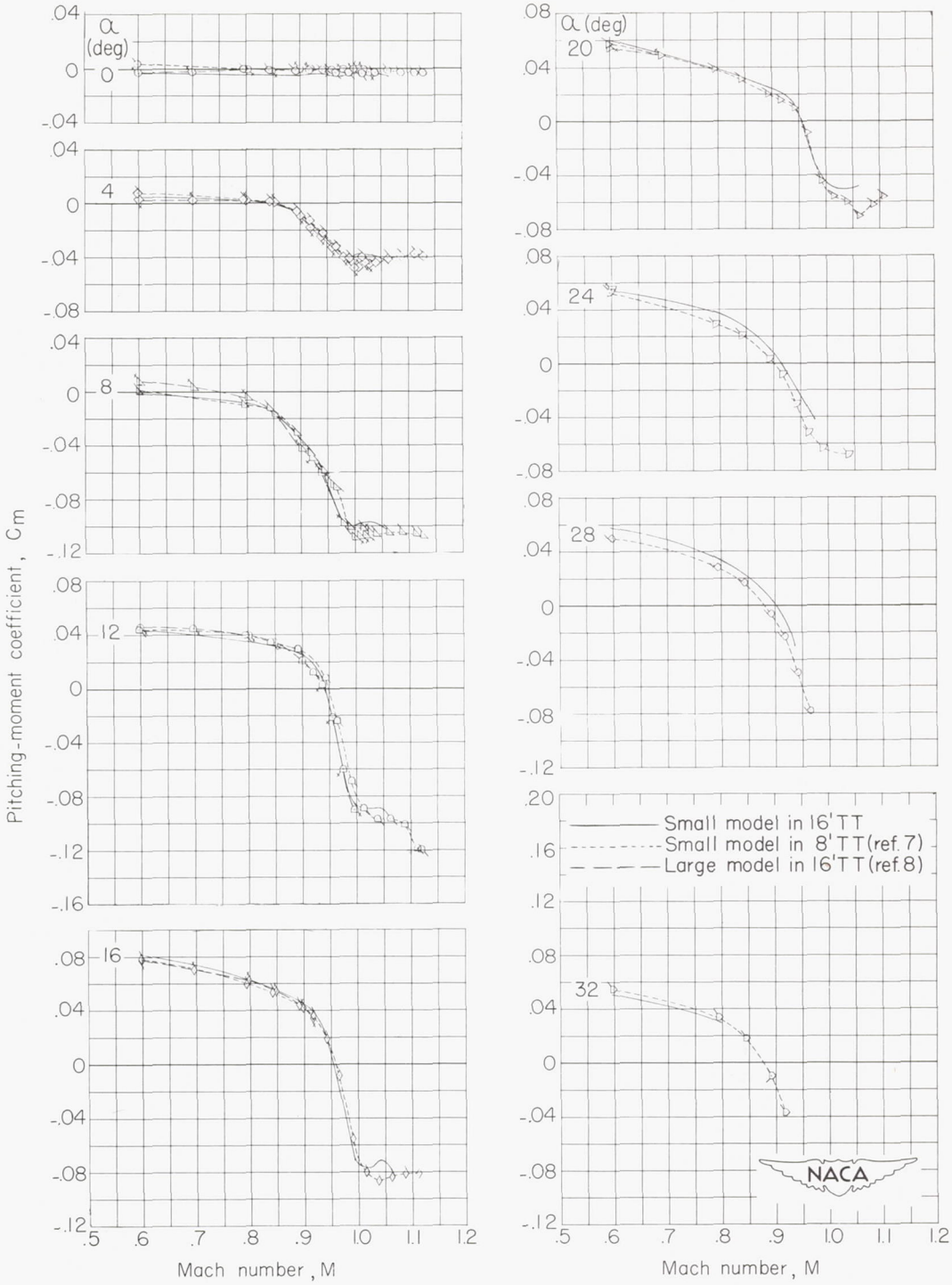

Figure 8.- Variation of pitching-moment coefficient with Mach number for the wing-fuselage configurations. (Single flagged symbols indicate data from small model in the Langley 8-foot transonic tunnel; cross-flagged symbols indicate data from the large model in the Langley 16-foot transonic tunnel.)

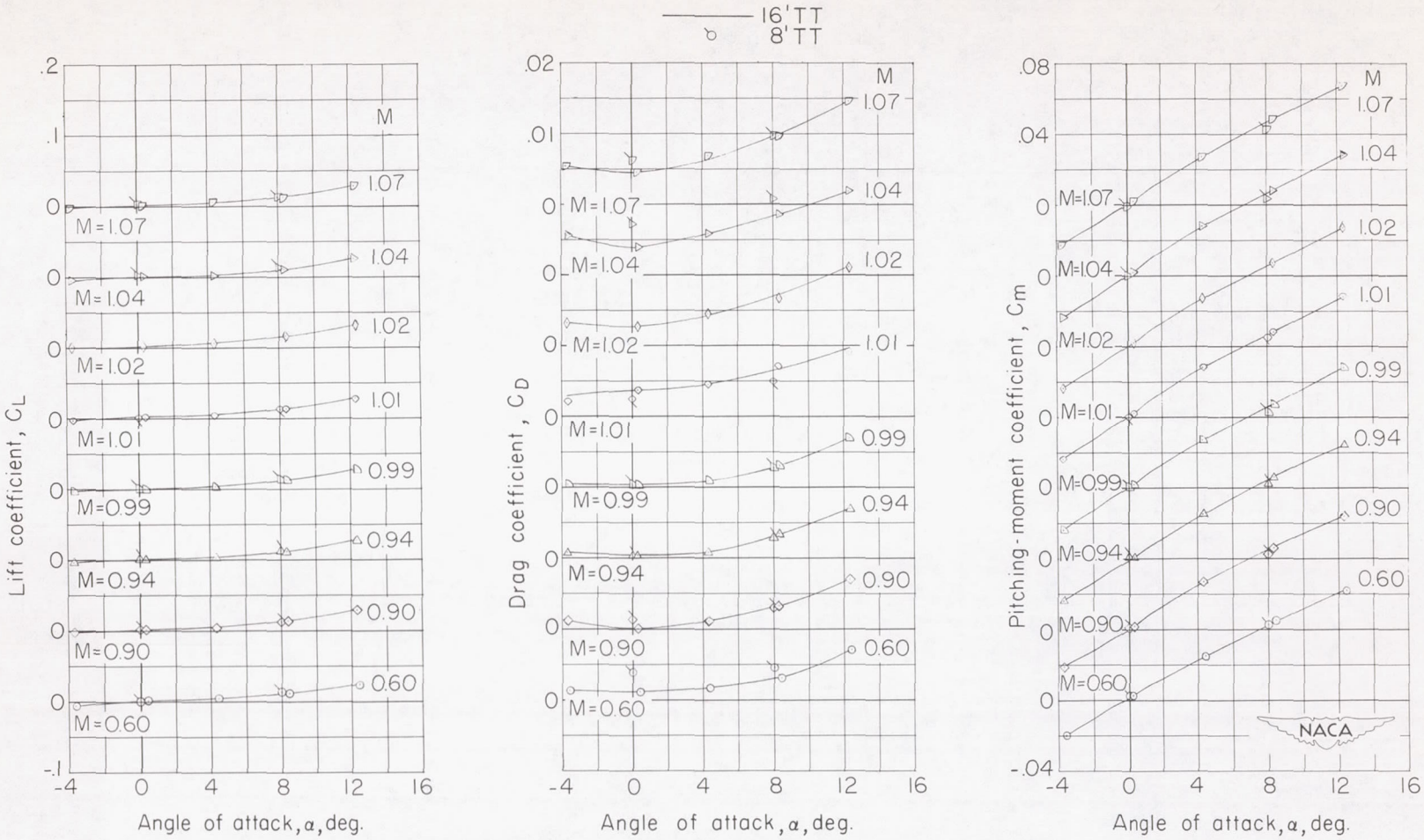

Figure 9.- Variation with angle of attack of force and moment characteristics of the small fuselage-alone model. (Plain symbols indicate data for model in the Langley 16-foot transonic tunnel; flagged symbols indicate data for model in the Langley 8-foot transonic tunnel.)

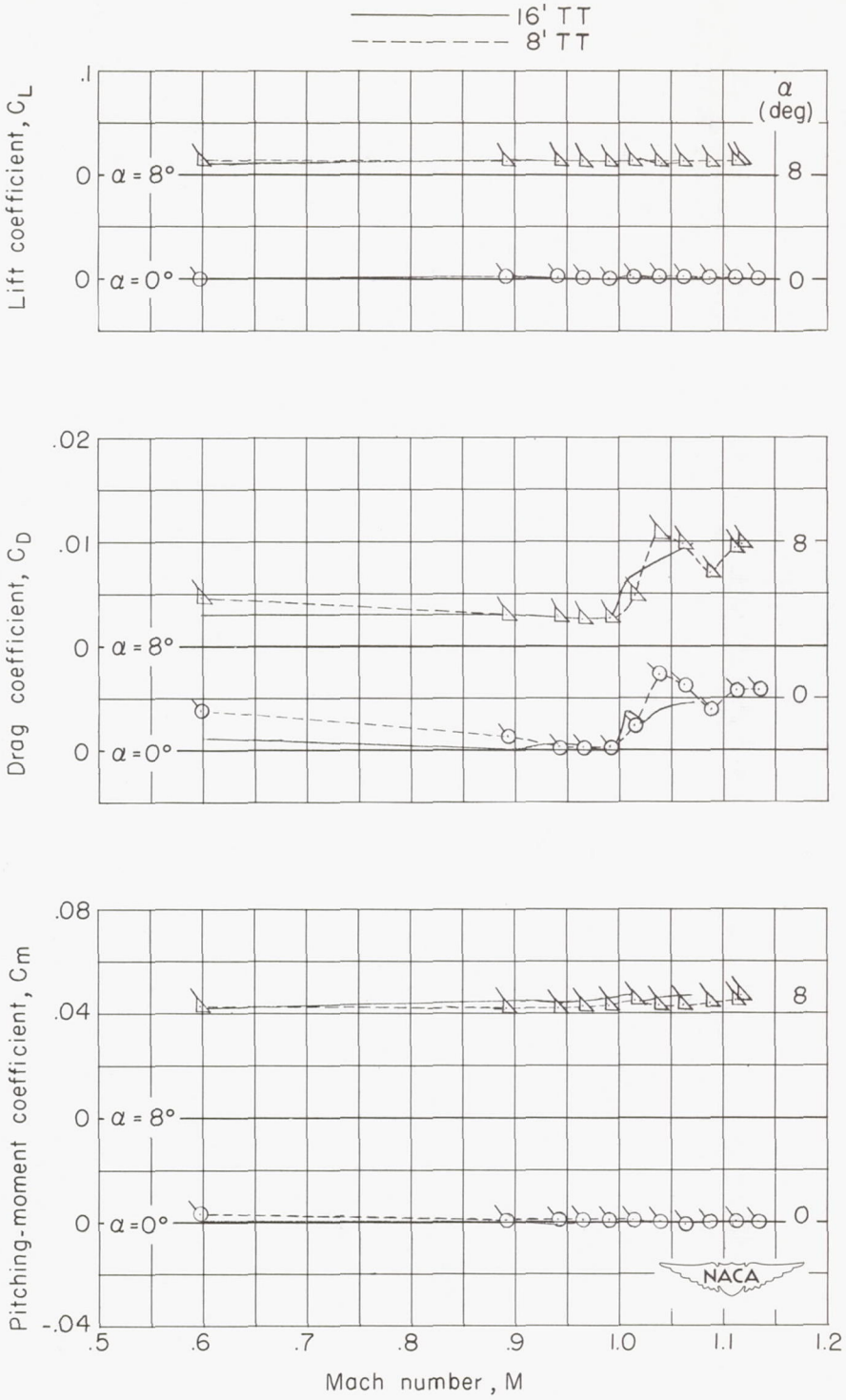

Figure 10.- Variation with Mach number of the force and moment characteristics of the small fuselage. (Flagged symbols indicate data for model in the Langley 8-foot transonic tunnel.)

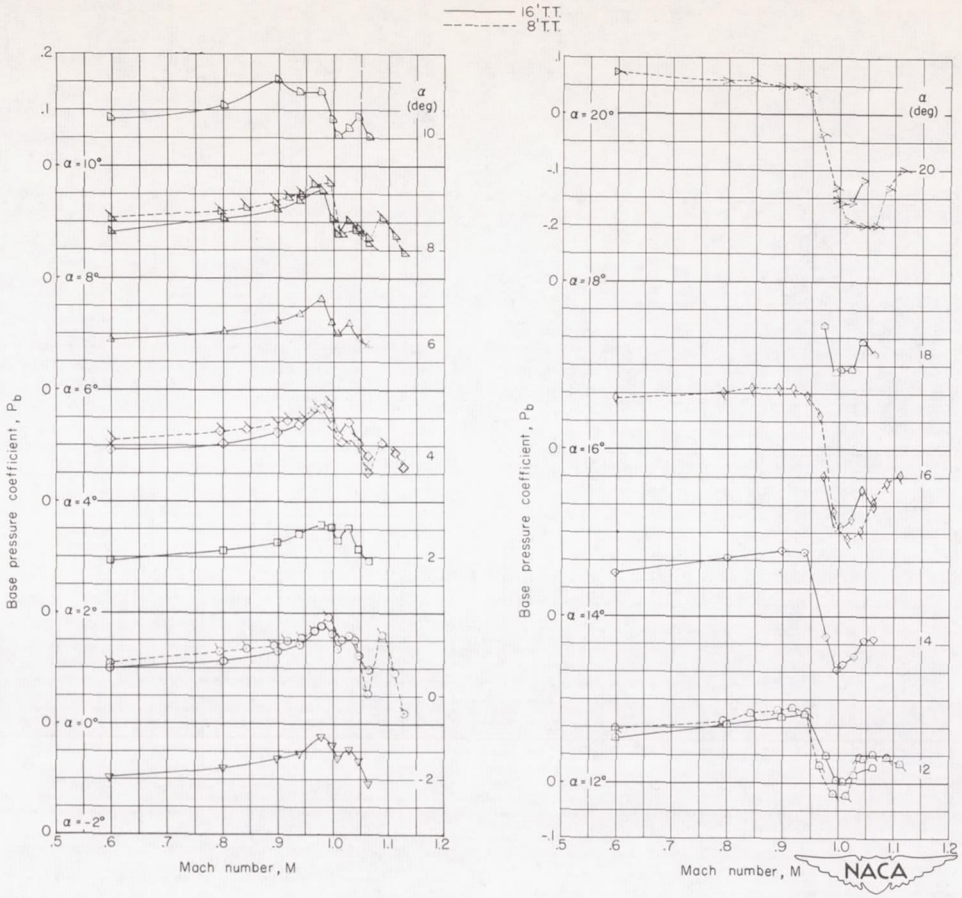

(a) Wing-fuselage combination.

Figure 11.- Variation of base pressure coefficients with Mach number for the fuselage and the wing-fuselage configurations of the small model. (Plain symbols indicate data for model in the Langley 16-foot transonic tunnel; flagged symbols indicate data for model in the Langley 8-foot transonic tunnel.)

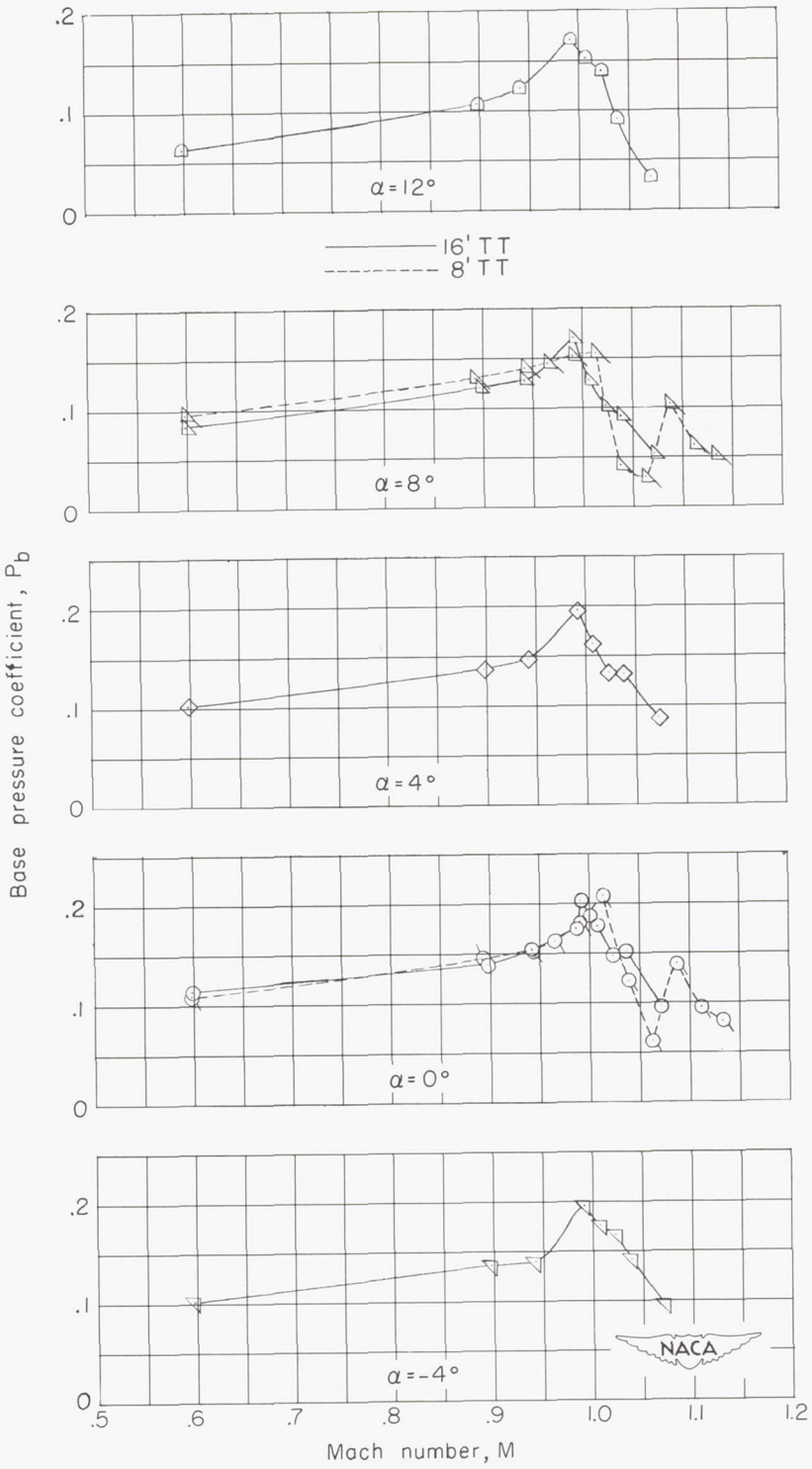

(b) Fuselage alone.

Figure 11.- Concluded.

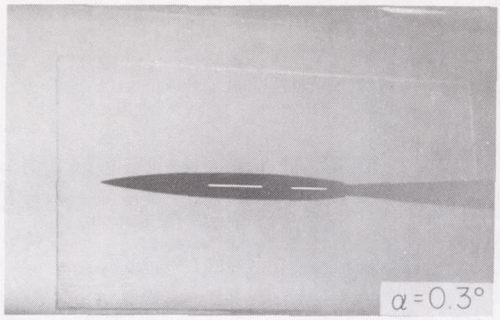

(a) M = 0.94.

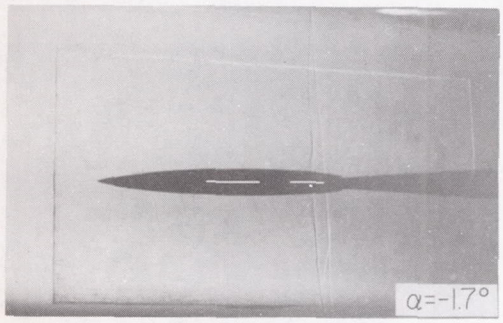

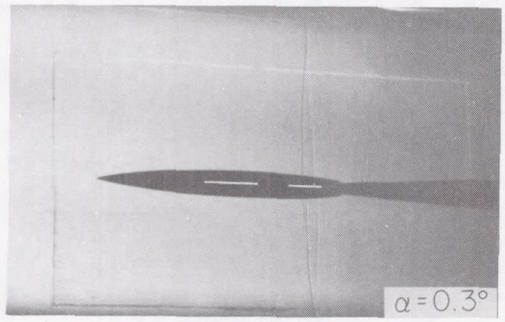

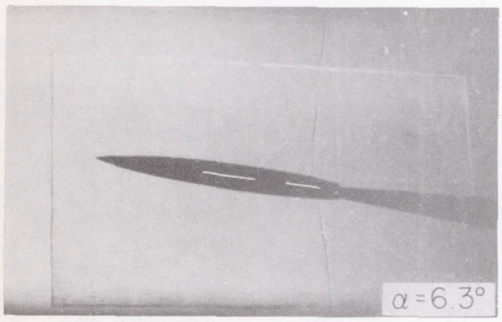

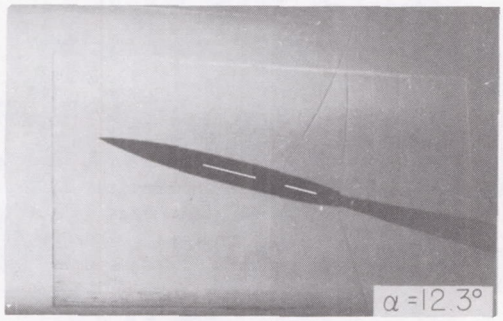

(b) M = 0.98.

L-77890

Figure 12.- Shadowgraph pictures of the small wing-fuselage configuration tested in the Langley 16-foot transonic tunnel at several Mach numbers.

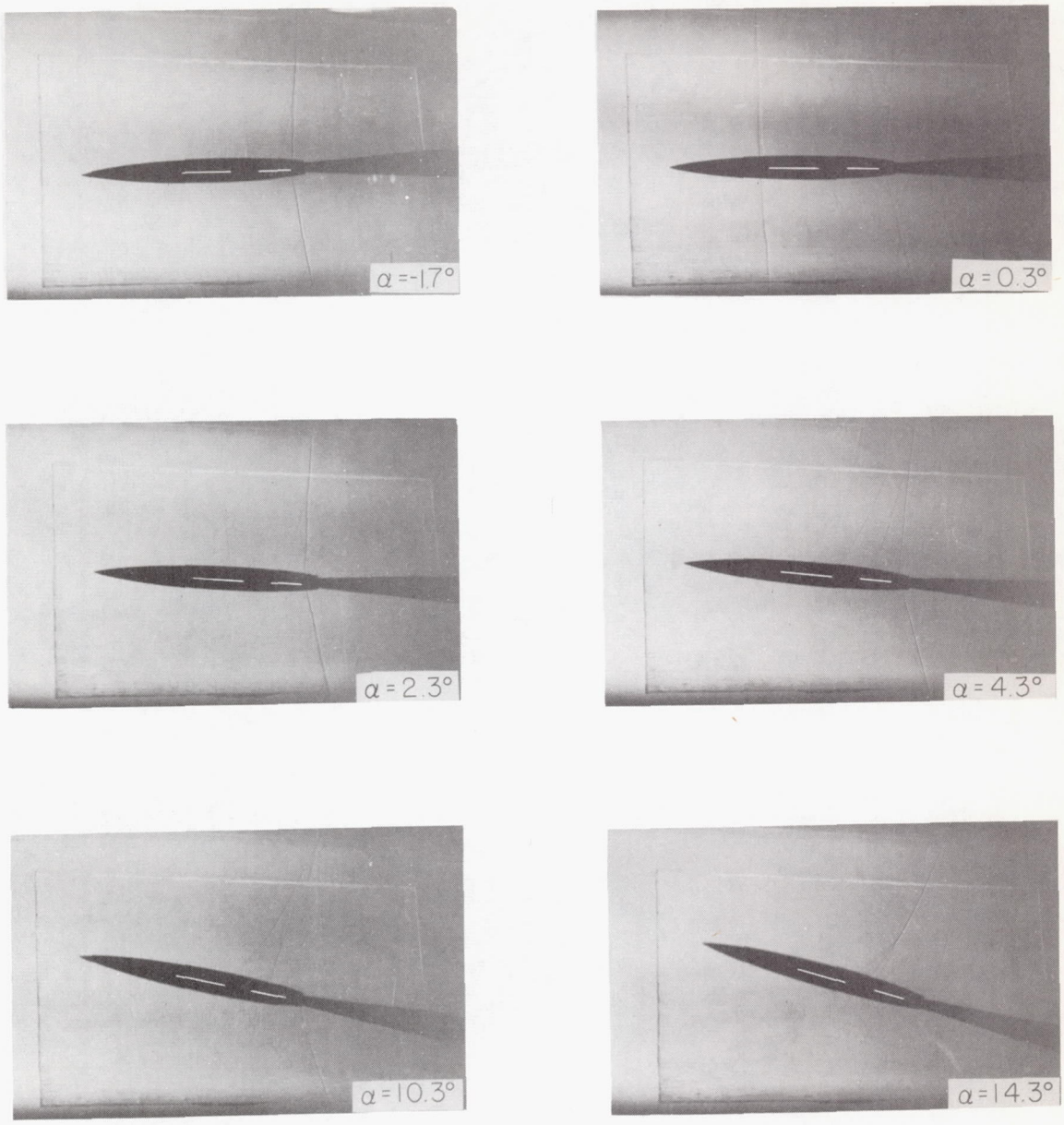

(c) M = 1.00.

NACA
L-77891

Figure 12.- Continued.

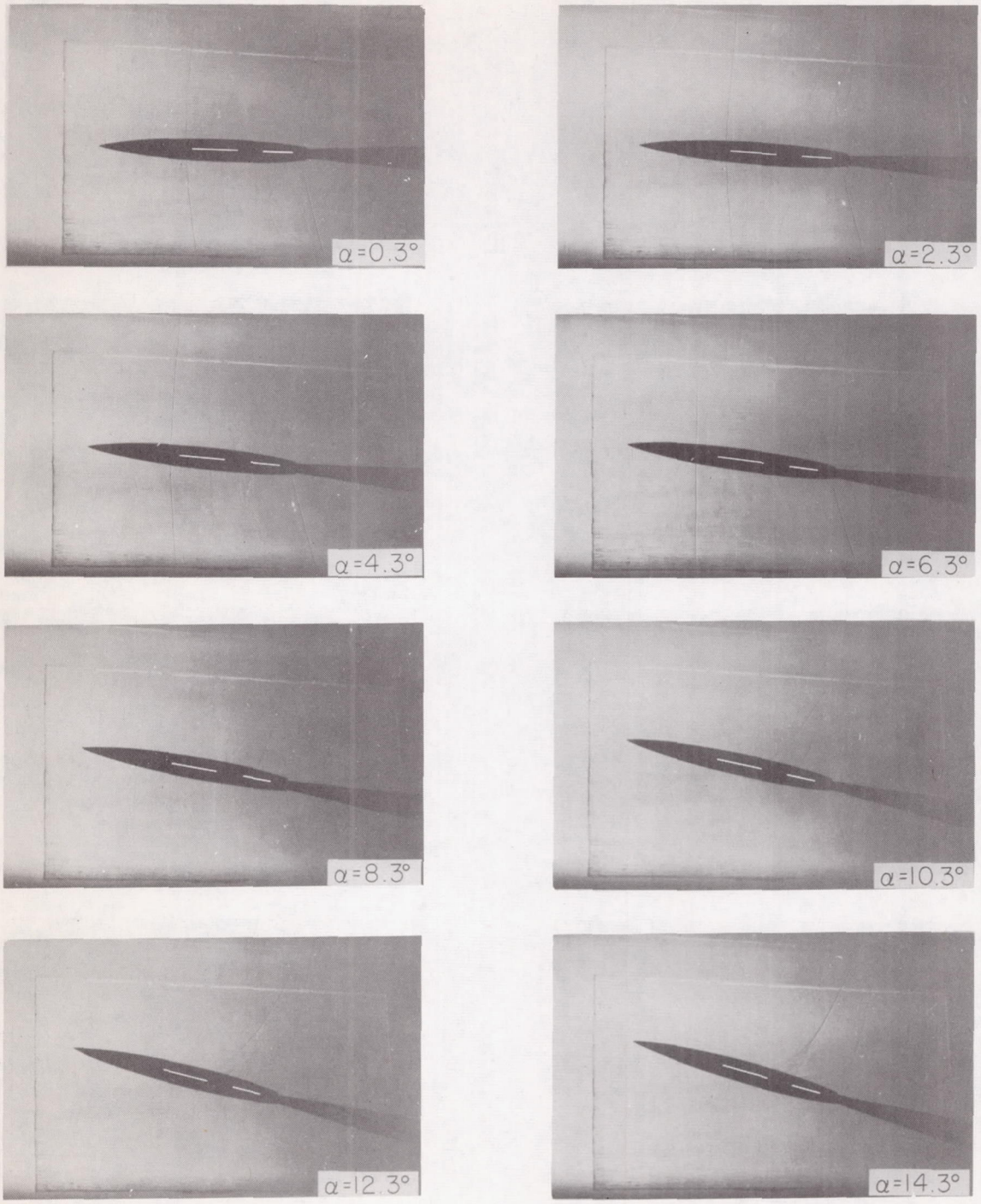

(d) M = 1.01.

Figure 12.- Continued.

NACA
L-77892

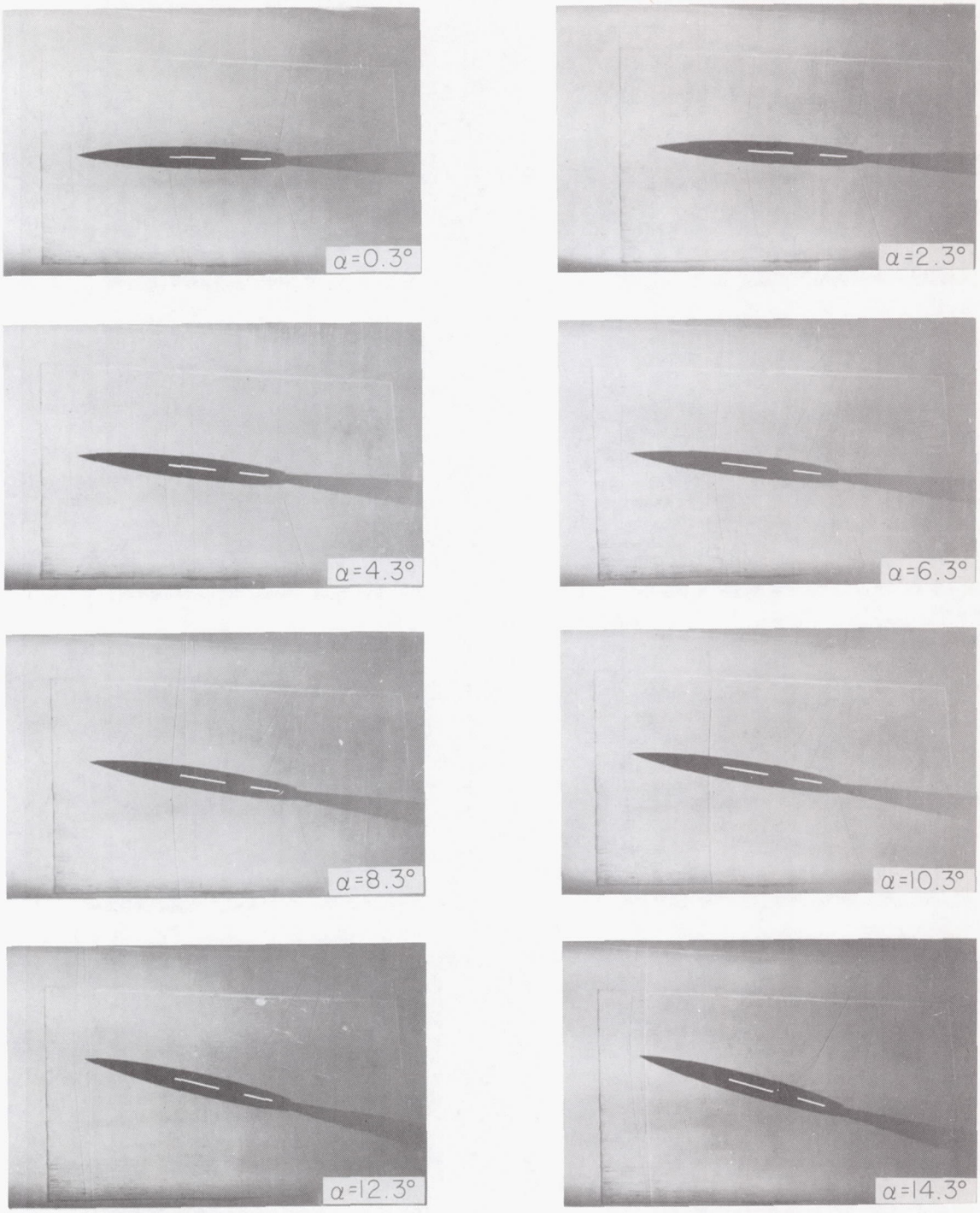

(e) M = 1.03.

Figure 12.- Continued.

NACA
L-77893

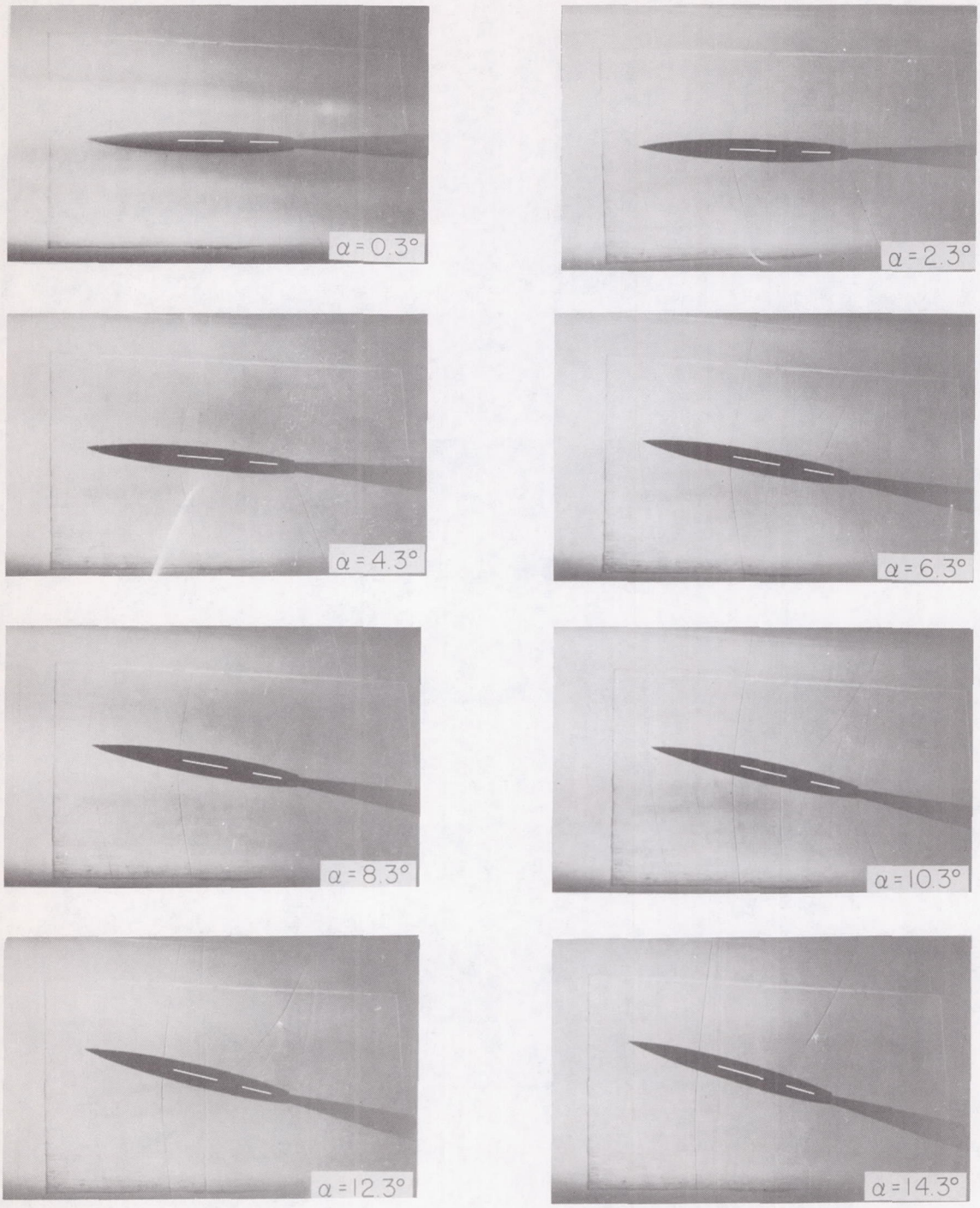

(f) M = 1.045.

NACA
L-77894

Figure 12.- Concluded.

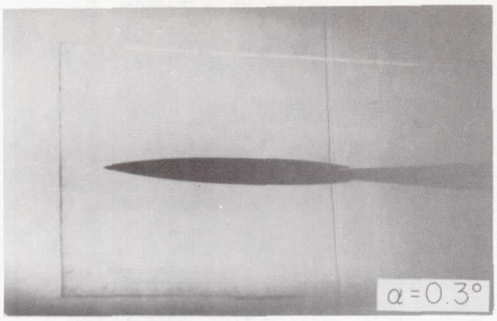

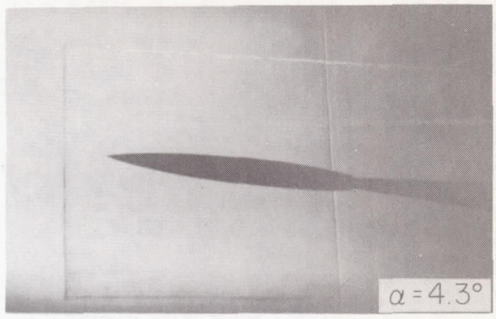

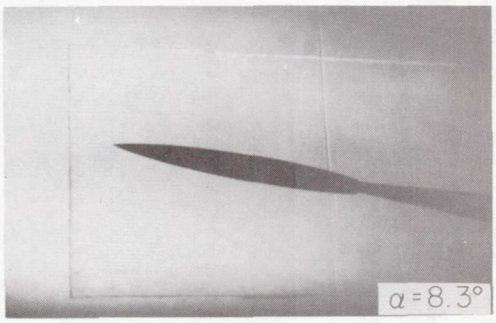

(a) M = 0.99.

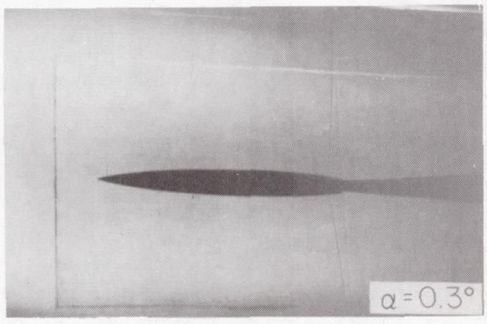

(b) M = 1.00.

NACA
L-77895

Figure 13.- Shadowgraph pictures of the small fuselage-alone configuration tested in the Langley 16-foot transonic tunnel at several Mach numbers.

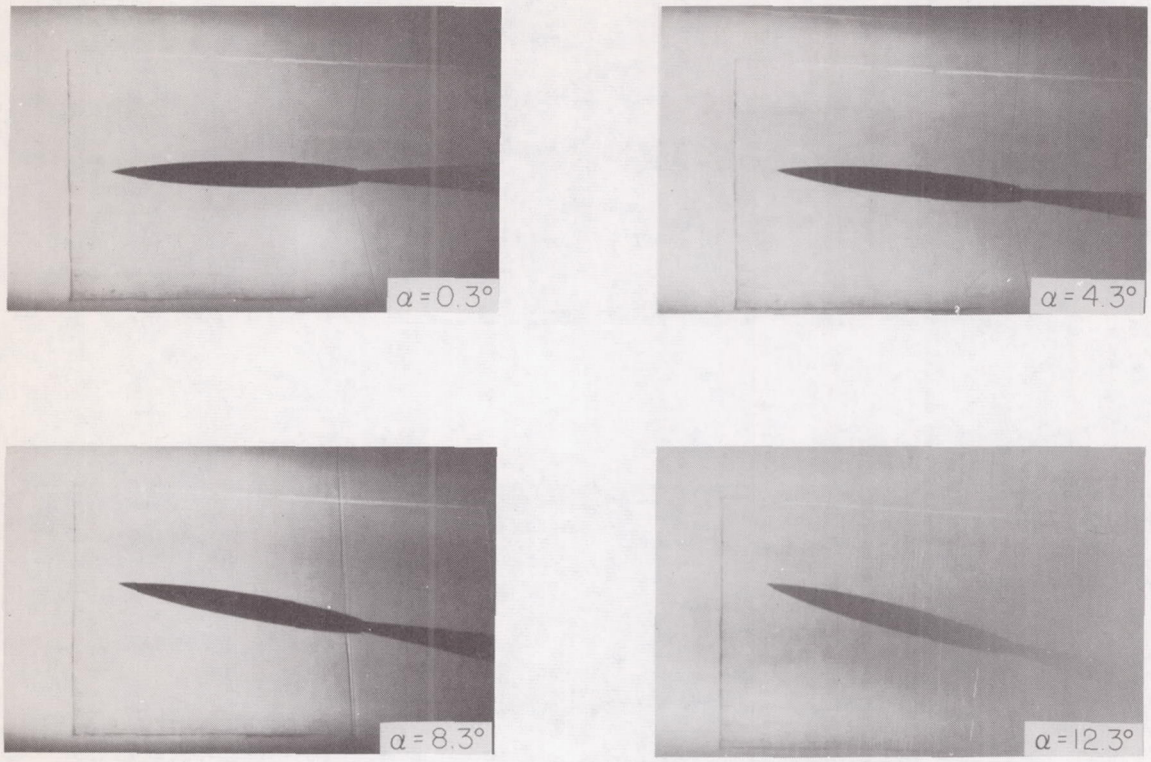

(c) M = 1.01.

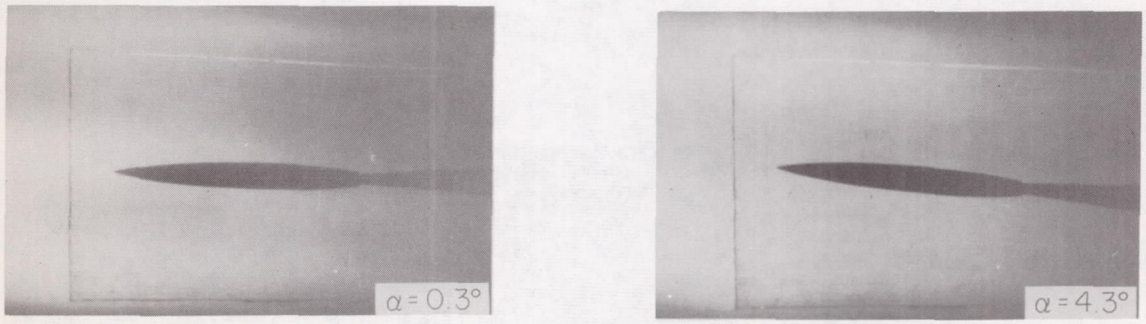

(d) M = 1.02.

NACA
L-77896

Figure 13.- Continued.

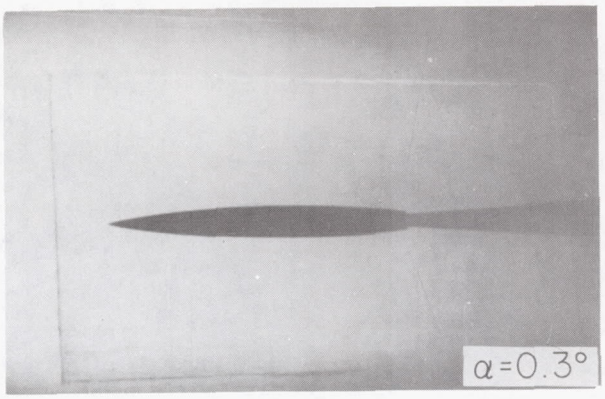

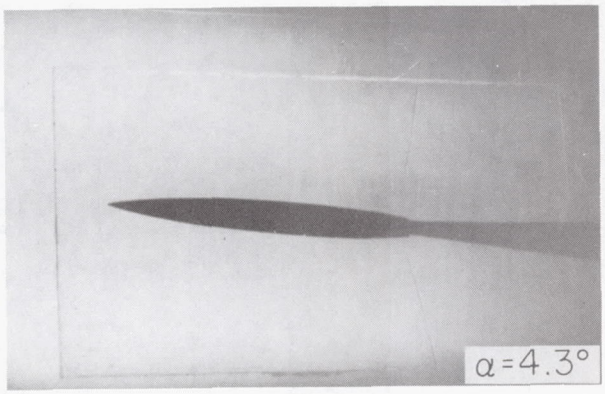

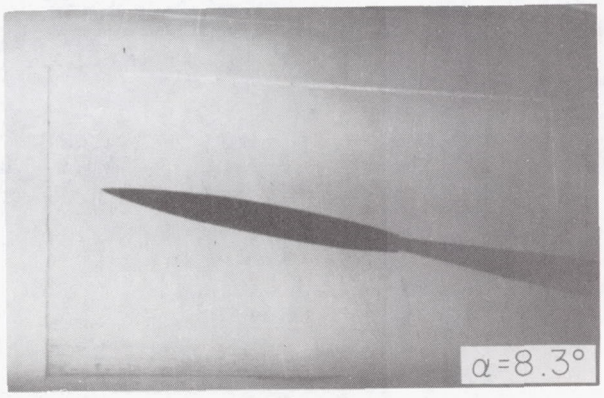

(e) M = 1.04.

Figure 13.- Continued.

NACA
L-77897

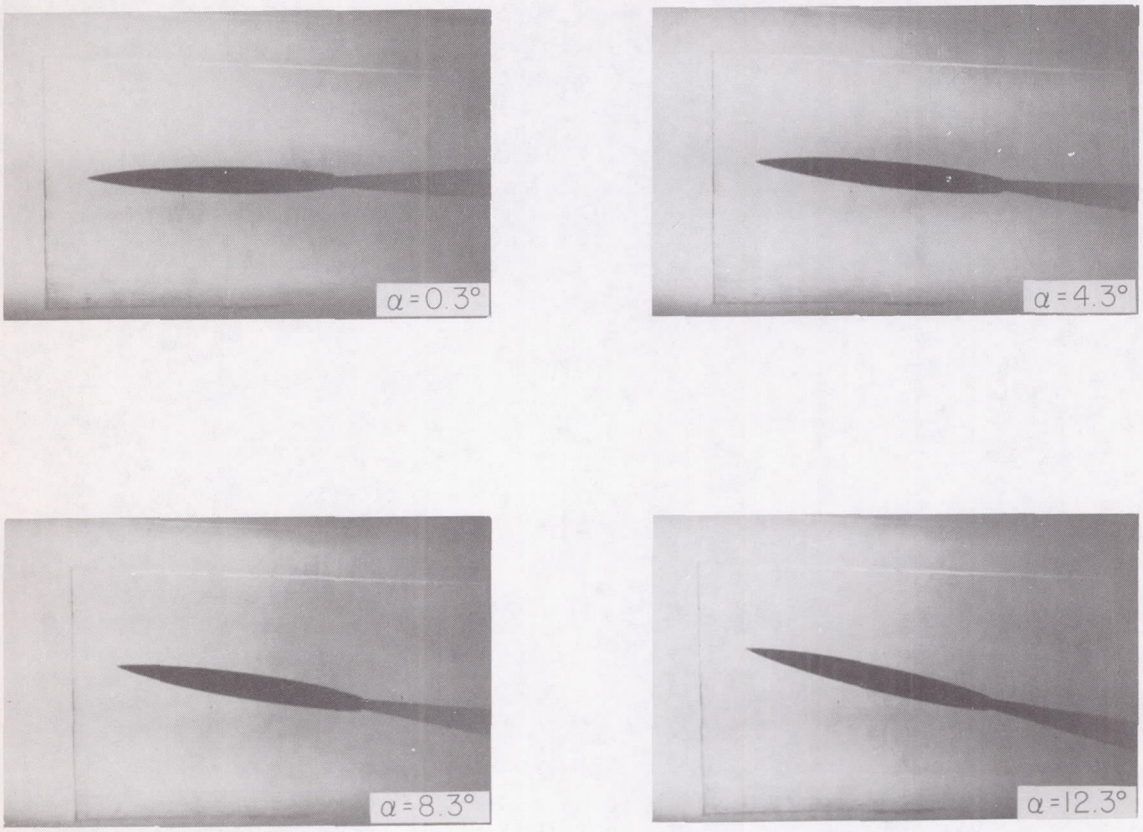

(f) M = 1.07.

L-77898

Figure 13.- Concluded.